ACS APPLIED MATERIALS & INTERFACES

Research Article

www.acsami.org

Novel Spirocyclic Phosphazene-Based Epoxy Resin for Halogen-Free Fire Resistance: Synthesis, Curing Behaviors, and Flammability Characteristics

Jian Sun, Xiaodong Wang,* and Dezhen Wu

State Key Laboratory of Organic−Inorganic Composite Materials, School of Materials Science and Engineering, Beijing University of Chemical Technology, Beijing 100029, China

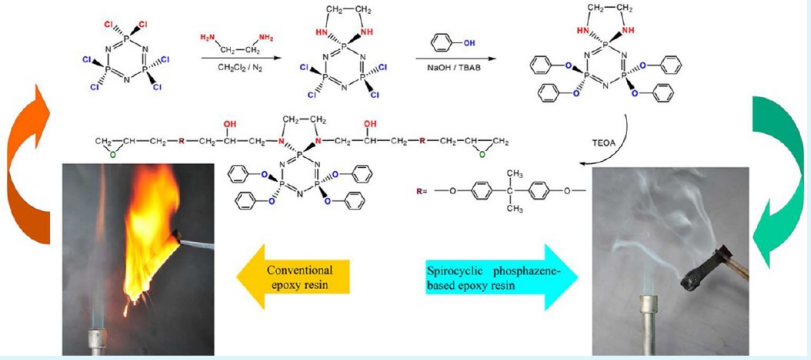

ABSTRACT: A novel halogen-free fire resistant epoxy resin with pendent spiro-cyclotriphosphazene groups was designed and synthesized via a three-step synthetic pathway. The chemical structures and compositions of spiro-cyclotriphosphazene precursors and final product were confirmed by ^{1}H, ^{13}C, and ^{31}P NMR spectroscopy, mass spectroscopy, elemental analysis, and Fourier transform infrared spectroscopy. The thermal curing behaviors of the synthesized epoxy resin with 4,4′-diamino-diphenylmethane, 4,4′-diamino-diphenyl sulfone, and novolac as hardeners were investigated by differential scanning calorimetry (DSC), and the curing kinetics were also studied under a nonisothermal condition. The evaluation of the thermal properties demonstrated that these thermosets achieved a good thermal resistance due to their high glass transition temperatures more than 150 °C, and also gained high thermal stabilities with high char yields. The flammability characteristics of the spirocyclic phosphazene-based epoxy thermosets cured with these three hardeners were investigated on the basis of the results obtained from the limiting oxygen index (LOI) and UL−94 vertical burning experiments as well as the analysis of the residual chars collected from the vertical burning tests. The high LOI values and UL−94 V−0 classification of these epoxy thermosets indicated that the incorporation of phosphazene rings into the backbone chain imparts nonflammability to the epoxy resin owing to the unique combination of phosphorus and nitrogen following by a synergistic effect on flame retardancy. The epoxy resin obtained in this study is a green functional polymer and will become a potential candidate for fire- and heat-resistant applications in electronic and microelectronic fields with more safety and excellent performance.

KEYWORDS: *spirocyclic phosphazene-based epoxy resin, synthesis, characterization, curing kinetics, thermal properties, flammability characteristics*

1. INTRODUCTION

Epoxy resins have been one of the most widely used materials in modern industrial areas due to their outstanding properties and great versatility. However, high flammability is one of the main drawbacks for epoxy resins, which greatly restricts their applications in many areas involved in electric and electronic industries.[1,2] In past decades, the halogen-containing epoxy resins like brominated ones have been developed to meet the considerable secure requirements. Especially in hi-tech electronic and microelectronic fields, the epoxy resins containing bromine atoms have particularly been useful for printed circuit boards and the encapsulation of semiconductor chips and devices, where fire resistance is absolutely desired.[3] However, major problems encountered with this system are concerned with the generation of toxic and corrosive fumes during combustion.[4] In recent years, the research and development of halogen-free fire-resistant epoxy resins have been attracting the increasing attention from both the scientific and industrial communities. It is absolutely undoubted that the simultaneous addition of phosphorus- and nitrogen-containing flame retardants is very effective way to impart a good fire-resistant property to epoxy resins as a result of the synergistically flame retarding effect.[5−8] Because the organo-phosphorus molecules are efficient radical scavengers and flame

Received: May 14, 2012
Accepted: July 25, 2012
Published: July 25, 2012

quenching materials, and combustion processes are essentially exothermic free-radical reactions, so the existence of radical stabilizers impedes combustion by the quenching mechanism.[9,10] On the other hand, the nitrogen-containing moieties that release inert gaseous byproduct to form a highly porous char that provides thermal insulation and prevents the combustion from spreading.[11−15] Nevertheless, there are still some problems that result in a limitation of their use in the electronic areas with a requirement of high performance. One of them is that the deterioration in thermal, electric, and mechanical properties is unacceptable for the fabrication of electronic parts and devices.[16] Therefore, the reactive approach, i.e., the incorporation of chemical units containing phosphorus, or nitrogen, or both into the macromolecular backbone or side chains, is considered as a more effective route, whose main advantage is to impart permanent flame retardancy as well as maintain the original physical properties of epoxy resins in a better way.[17−22] Many studies have been reported for the design and synthesis of flame retardant epoxy resins by incorporating phosphorus-containing flame retarding units in their backbone such as phosphine oxide, phosphates, and the other phosphorylated and phosphonylated derivatives.[20−23] However, these phosphorus-containing epoxy resins hardly gain high weight fraction of phosphorus, resulting in a low degree of flame retardancy. Currently, a great interest is focusing on the redesign of both the backbone and the side chains of epoxy resins with more highly flame retarding moieties.

It has been reported that the phosphazene materials usually possess good physical properties and high thermooxidative stability as well as excellent flame retardancy.[24−27] The chemical incorporation of cyclotriphosphazene units into the epoxy resins is considered as a good idea to gain a dramatically high flame retarding efficiency and autoextinguishability due to the synergistic effect derived from the skeletal phosphorus and nitrogen atoms of cyclotriphosphazene moieties.[28,29] In most cases, cyclotriphosphazene-containing polymers are synthesized from commercially available hexachlorocyclotriphosphazene ($N_3P_3Cl_6$), which can be readily modified with a variety of substituents via a nucleophilic substitution. The good reactivity of replaceable chlorine atoms linked to the phosphorus atoms of a phosphazene ring offers synthetic adaptability to introduce a large number of substituents with appropriate functionality, which can subsequently be transformed into desired synthetic precursors.[30−33] Therefore, the synthesis of phosphazene-based epoxy resins is expected to be feasible and facile. Some reported investigations show that epoxy thermosetting resins containing cyclotriphosphazene units exhibit a potential application in the electronic industry for their good flame retardancy and high thermal resistance.[34−37] So it is desirable to use this synergistic approach to obtain novel halogen-free flame retardant epoxy materials with high performance.

In this study, we designed and synthesized a novel spirocyclic phosphazene-based epoxy resin for halogen-free flame retardancy. Such a cyclotriphosphazene moiety with the spiro-side group will have a higher content of the phosphazene component than counterparts with linear side groups, because the former requires only three substituents per phosphazene ring while the latter requires six.[38,39] This indicates that replacement of chlorine atoms in cyclotriphosphazene in a spirocyclic mode is an effective method for the synthesis of phosphazene-based epoxy resins with a high phosphorus−nitrogen content leading to higher flame retardancy. The incorporation of spiro-cyclotriphosphazene moieties into the backbone is expected to enhance the thermal resistance, thermal stability, and most importantly, much better fire resistance of the resulting epoxy resins. A complementary study on the curing behaviors and flammability characteristics of this epoxy resin was also performed and described in this article.

2. EXPERIMENTAL SECTION

2.1. Chemicals. Hexachlorocyclotriphosphazene (**1**) was commercially obtained from Shanghai Yagu Chemical Co., Ltd., China. It was purified by recrystallization from *n*-heptane followed by a vacuum sublimation (60 °C and 0.05 mmHg) before use. Ethylenediamine (**2**), phenol (**4**), tetrabutyl ammonium bromide (TBAB), triethanolamine (TEOA), sodium hydroxide (NaOH), dichloromethane (CH_2Cl_2), tetrahydrofuran (THF), and *n*-hexane were purchased from Beijing Chemical Reagent Co., Ltd., China. The solvents used, CH_2Cl_2 and *n*-hexane, were dried by anhydrous sodium sulfate (Na_2SO_4) prior to use, and the other chemicals and reagents were used as received. Diglycidyl ether of bisphenol A (**6**, DGEBA) was commercially supplied by Wuxi Dic Epoxy Co., Ltd. 4,4′-Diamino-diphenylmethane (DDM), 4,4′-Diamino-diphenyl sulfone (DDS), and novolac were selected as hardeners and also purchased from Beijing Chemical Reagent Co., Ltd., China.

2.2. Synthesis and Reactions. *2.2.1. Synthesis of 1,1-Spiro-(ethylenediamino)-3,3,5,5-tetrachloro -cyclotriphosphazene (**3**).* A 500 mL three-necked round-bottom flask equipped with a reflux condenser, a nitrogen inlet, and a dropping funnel was charged with a solution of **1** (28 g, 0.08 mol) in CH_2Cl_2 (200 mL). A solution of **2** (11 mL, 0.16 mol) in CH_2Cl_2 (50 mL) was added dropwise into the flask over 1 h with agitation, followed by stirring for 1 h under a nitrogen atmosphere. After the reaction was completed, the reaction mixture was filtered and then washed repeatedly with hot water. The organic layer separated was dried with anhydrous Na_2SO_4 and concentrated on a rotatory evaporator under reduced pressure. The remaining crude product was recrystallized from $CHCl_3$ to give a white crystalline solid of **3** (22.19 g, yield 82.9%). ^{1}H NMR ($CDCl_3$): δ = 3.46 (d, 4H) and 2.76 ppm (s, 2H). ^{13}C NMR ($CDCl_3$): δ = 42.30 ppm (s, 2C). ^{31}P NMR ($CDCl_3$): δ = 26.08 (d, 2P) and 21.50 ppm (t, 1P). MS: m/z = 335.8 $[M+1]^+$. Elemental anal. Found: C, 7.48; H, 1.76; N, 20.63. Calcd for $C_2H_6Cl_4N_5P_3$: C, 7.17; H, 1.81; N, 20.92. FTIR (KBr): ν (N−H): 3,356 cm^{-1}, ν (C−H): 2,884 cm^{-1}, ν (P═N): 1,232 cm^{-1}, ν (P−N): 833 cm^{-1}, and ν (P−Cl): 534 cm^{-1}.

*2.2.2. Synthesis of 1,1-Spiro(ethylenediamino)-3,3,5,5-tetra-(phenoxy)-cyclotriphosphazene (**5**).* NaOH (9.84 g, 0.25 mol), **4** (11.58 g, 0.125 mol), and TBAB as a phase-transfer catalyst (1.19 g, 3.75 mmol) were dissolved in deionized water (200 mL) in a round-bottom flask equipped with a dropping funnel and a magnetic stirring bar, and the reaction mixture was cooled with an ice bath. Sequentially, a solution of **3** (8.23 g, 0.025 mol) in CH_2Cl_2 (150 mL) was added dropwise into the flask over 30 min, and then the reaction mixture was vigorously stirred at room temperature for 24 h under a nitrogen atmosphere. After the reaction was completed, the reaction mixture was filtered, washed repeatedly with hot water, and then dried with anhydrous Na_2SO_4. The solvent was removed by rotatory evaporation under reduced pressure, leaving a white solid. Ultimately, the white solid was further purified by column chromatography (silica gel, THF:*n*-hexane = 2:1), and the removal of solvent gave a colorless crystalline solid of **5** (12.6 g, yield 90.6%). ^{1}H NMR ($CDCl_3$): δ = 7.31 (t, 8H), 7.15 (t, 4H), 7.03 (d, 8H), 3.25 (d, 4H), and 1.87 ppm (s, 2H). ^{13}C NMR ($CDCl_3$): δ = 151.00 (s, 4C), 129.37 (s, 8C), 124.76 (s, 4C), 121.23 (s, 8C), and 42.35 ppm (s, 2C). ^{31}P NMR ($CDCl_3$): δ = 32.48 (t, 1P) and 10.54 ppm (d, 2P). MS: m/z = 566.2 $[M+1]^+$. Elemental anal. Found: C, 56.17; H, 4.81; N, 12.46. Calcd for $C_{26}H_{26}N_5O_4P_3$: C, 55.23; H, 4.63; N, 12.39. FTIR (KBr): ν (N−H): 3410 cm^{-1}, ν (Ph−H): 3,067 cm^{-1}, ν (C−H): 2,891 cm^{-1}, ν (C−N): 1105 cm^{-1}, ν (C═C): 1,592 and 1,488 cm^{-1}, ν (P═N): 1,258 and 1,198 cm^{-1}, ν (P−N): 853 cm^{-1}, and ν (P−O−Ph): 940 cm^{-1}.

*2.2.3. Synthesis of Spirocyclic Phosphazene-Based Epoxy Resin (**7**).* A 250 mL round-bottom flask with a stirrer, reflux condenser and nitrogen inlet was charged with **5** (49.5 g, 0.09 mol). The compound

Scheme 1. Synthetic Reaction for the Formation of Spiro-Cyclotriphosphazene Precursor 3

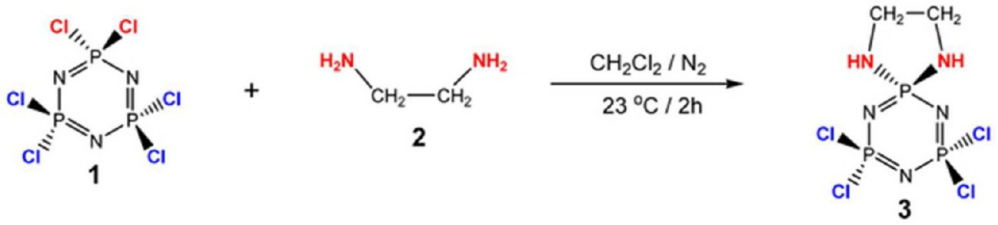

was heated to 120 °C and kept at this temperature for 1 h with agitation to remove all the volatile impurities. To this compound, **6** (30.0 g, 0.18 mol) and TEOA (1.48 g, 0.01 mol) as a catalyst were added, and then the reaction mixture was stirred at 150 °C for 3 h. When the reaction finished, the reaction mixture was cooled to room temperature, and afforded **7** as a brown viscous liquid. ^{1}H NMR ($CDCl_3$): δ=7.40−6.60 (m, aromatic H), 4.18 (d, 2H), 4.16 (d, 2H), 3.96 (m, 4H), 3.95 (m, 2H), 3.92 (m, 2H), 3.59 (s, 2H), 3.33 (m, 2H), 3.22 (d, 4H), 2.93 (s, 6H), 2.89 (m, 2H), 2.87 (m, 2H), 2.74 (m, 2H), 1.63 ppm (s, 12H). ^{13}C NMR ($CDCl_3$): δ = 156.36 (s, 4C), δ = 150.57 (s, 4C), δ = 143.66 (s, 4C), δ = 129.53 (s, 8C), δ = 127.80 (s, 8C), δ = 124.79 (s, 4C), δ = 121.24 (s, 8C), δ = 114.03 (s, 8C), δ = 73.65 (s, 2C), δ = 68.77 (s, 2C), δ=66.9 (s, 2C), δ = 50.23 (s, 2C), δ = 46.05 (s, 2C), δ = 44.78 (s, 2C), δ = 42.40 (s, 2C), δ = 41.75 (s, 2C) and 31.05 ppm (s, 4C). ^{31}P NMR ($CDCl_3$): δ = 31.77 (t, 1P) and 10.57 ppm (d, 2P). Elemental anal. Found: C, 65.17; H, 5.93; N, 5.64. Calcd for $C_{68}H_{24}N_5O_{12}P_3$: C, 65.53; H, 5.98; N, 5.62. FTIR (KBr): ν (−OH): 3,402 cm^{-1}, ν (Ph−H): 3,081 cm^{-1}, ν (−CH_3): 2,957 cm^{-1}, ν (−CH_2): 2,887 cm^{-1}, ν (C═C): 1,613, 1,590, 1520 and 1,487 cm^{-1}, ν (P═N): 1,241 and 1,215 cm^{-1}, ν (C(CH_3)$_2$): 1350 cm^{-1}, ν (P−O−Ph): 1175 cm^{-1}, ν (C−N): 1103 cm^{-1}, ν (P−N): 855 cm^{-1} and ν (C−O−C): 919 cm^{-1}.

2.3. Curing Procedure of Spirocyclic Phosphazene-Based Epoxy Resin. The synthesized spirocyclic phosphazene-based epoxy resin was cured using DDM, DDS, and novolac as hardeners. The spirocyclic phosphazene-based epoxy resin was dissolved in appropriate amount of acetone, and then the hardener was added with an equivalent ratio to the epoxy resin of 1:1. 2-Methylimidazole (0.2 wt. %) as a curing accelerator was also added into this solution. The mixture was stirred constantly to be a homogeneous solution and then was kept in a vacuum oven at 90 °C for 3 h to remove the solvent. A two-step curing procedure was carried out in a mold to obtain the thermosetting resins. The epoxy formulations containing DDM, DDS, and novolac were first precured at 140, 150, and 150 °C, respectively, for 2 h, and then were further postcured at 180 °C for 3 h. In the end of the curing procedure, the cured system was cooled gradually to room temperature to avoid stress crack.

2.4. Characterization. *2.4.1. Nuclear Magnetic Resonance (NMR) Spectroscopy.* ^{1}H, ^{13}C and ^{31}P NMR spectra of the synthesized spiro-cyclotriphosphazene precursors and final product targeted were obtained using a Bruker AV-400 400 MHz spectrometer in deuterochloroform ($CDCl_3$) solution, and were referenced to external tetramethylsilane (TMS) and 85% H_3PO_4 with positive shifts recorded downfield from the reference. The ^{13}C and ^{31}P NMR spectra were proton decoupled.

2.4.2. Mass Spectroscopy. The mass spectra were recorded on a Waters Quattro XE mass spectrometer. Electrospray ionization was used for the mass spectra with 25 EV and the mass range of 10−1000 m/z.

2.4.3. Elemental Analysis. The elemental analysis was performed with a Vario−EL−cube CHNS elemental analyzer (Elementar Analysensysteme GmbH).

2.4.4. Fourier Transform Infrared (FTIR) Spectroscopy. FTIR spectra were obtained using a Bruker Tensor−27 FTIR spectrometer with a scanning number of 50. A finely ground, approximately 1% mixture of a solid sample in KBr powders is fused into a transparent disk for FTIR measurement using a hydraulic press.

2.4.5. Epoxy Equivalent Weight Measurement. The epoxy equivalent weight (EEW) of the synthesized cyclolinear phosphazene-based epoxy resin was determined by the HCl/acetone chemical titration method.

2.4.6. Steric Exclusion Chromatography Measurement. The molecular weight and its distribution were obtained through steric exclusion chromatography (SEC) using a Waters GPC515−2410 gel permeation chromatographer equipped with a Waters 515 pump, a Waters 2489 UV/visible light detector, and a Waters 2414 refractive index detector. The sample (6−8 mg) was first dissolved in 1 mL of THF, and then was eluted with THF as solvent through a series of Styragel chromatographic columns (HR0.5, HR1, HR2, and HR4E) at a flow rate of 1.0 mL/min. Such a set of the chromatographic columns covered the measurable range of molecular weight from 100 to 100 000, and all of them were calibrated with narrow molecular weight distribution polystyrene standards.

2.4.7. Differential Scanning Calorimetry (DSC). The thermal curing study of the epoxy resin with various hardeners was carried out on a TA Instruments Q20 differential scanning calorimeter equipped with a thermal analysis data station, operating at heating rates of 5, 10, 15, and 20 °C/min under a nitrogen atmosphere. Thermal transition temperatures were also determined by DSC.

2.4.8. Thermogravimetric Analysis (TGA). TGA measurements were performed under a nitrogen atmosphere using a TA Instruments Q50 thermal gravimetric analyzer. The samples with a mass of about 10 mg were placed in an aluminum crucible, and ramped from room temperature up to about 800 °C at a heating rate of 10 °C/min, whereas the flow of nitrogen was maintained at 50 mL/min.

2.4.9. Limiting Oxygen Index Test (LOI). LOI tests were performed using a HD−2 oxygen index apparatus with a magneto-dynamic oxygen analyzer, according to the ASTM D−2863 standard. The mixture of oxygen and nitrogen gas was continuously passed through the combustion chamber at a flow rate of 170 mL/min. The sample bar with a dimension of 65 × 3.0 × 1.6 mm was clamped vertically in the holder in the center of the combustion column. The top of the sample bar was ignited using a butane gas burner so that the sample bar was well lit and the entire top was burning. The relative flammability of the sample bar was determined by measuring the minimum concentration of oxygen, which would just support flaming combustion of the sample bar.

2.4.10. UL-94 Vertical Burning Test. UL−94 vertical burning experiments were carried out based on the testing method proposed by Underwriter Laboratory according to ASTM D−1356/2002 standard. Five test sample bars with a dimension of 127 × 12.7 × 1.6 mm suspended vertically over surgical cotton were ignited using a butane gas burner. The end of the sample bar was ignited twice, and each ignition was carried out for 10 s. The classification of V−0 is obtained if the burning time of each sample bar after 10-s ignition does not exceed 10 s, and the total burning time for five samples does not exceed 50 s; at the same time, the surgical cotton below the specimen cannot be ignited by the flaming drippings.

2.4.11. Scanning Electron Microscopy (SEM). The SEM observation was performed on a Hitachi S−4700 scanning electron microscope to investigate the morphologies of the residual chars. The char samples for SEM were obtained after combustion in the vertical burning tests and were made electrically conductive by sputter coating with a thin layer of gold−palladium alloy. The images were

Scheme 2. Synthetic Reaction for the Formation of Spiro-Cyclotriphosphazene Precursor 5

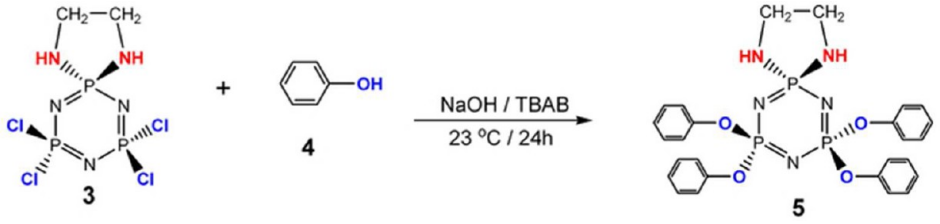

taken in high vacuum mode with 20 kV acceleration voltage and a medium spot size.

3. RESULTS AND DISCUSSION

3.1. Synthesis and Characterization. To obtain the spirocyclic phosphazene-based epoxy resin, three step reactions have been performed as shown in Schemes 1−3, where the synthetic pathway and the structural features of spiro-phosphazene precursors and final product are clearly illustrated. As is shown by Scheme 1, the synthesis of the monospiro-substituted phosphazene precursor **3** is straightforward and utilizes the reaction of a commercial product **1** with a diamine **2** in the presence of base as a hydrochloride accelerator. A geminal attack by primary amino groups is known to be favored in this medium. To avoid side reactions, we slowly added a dilute solution of **2** dropwise to a dilute solution of **1**. Although the reactivity of the diamine decreased significantly as the size of the organic group increased, this reaction was completed within 2 h at room temperature in a good yield of final product. The ^{1}H, ^{13}C, and ^{31}P NMR spectroscopy has well-characterized the structure of **3** as described in the Experimental Section. Additionally, the mass spectrum and elemental analysis results (see Experimental Section) are in good agreement with the data calculated in light of the expected formula of 3. These characterization data further indicated that the monospiro-substituted phosphazene precursor were successfully synthesized, and no side products were detected.

The reaction route used to synthesize the tetraphenoxy-substituted spiro-phosphazene precursor **5** is also straightforward. As is shown by Scheme 2, the monospiro-substituted phosphazene precursor **3** was conveniently reacted with **4** by a typical interfacial condensation reaction in the presence of a phase-transfer catalyst, TBAB, using sodium phenolate in water as an aqueous phase and **4** in CH_2Cl_2 as an organic phase, and the pure compound targeted to obtain could be isolated by column chromatography. The chemical structure of **5** was monitored by ^{1}H, ^{13}C, and ^{31}P NMR spectroscopy. It is observed from Figure 1 that the ^{31}P NMR spectrum of **5** clearly displays a typical AB_2 spin pattern with two sets of resonance signals appearing as a triplet at 32.48 and as a doublet at 10.54 ppm, corresponding to the phosphorus atom of cyclotriphosphazene bearing a monospiro group and the other two bearing phenol groups, respectively. These two different environmental phosphorus atoms, i.e., P*−$(OC_6H_5)_2$ and P*$_{spiro}$−(HNC_2H_4NH), give an integration ratio of 2:1. Meanwhile, the spectrum of **1** as a reference shows only an intensive singlet signal at 19.97 ppm. The ^{1}H NMR spectrum shows several sets of resonance signals, which are well-assigned to all the protons of **5** as explicated in Figure 2, where the chemical shifts at 7.4−7.0 ppm are attributed to the aromatic protons on phenoxy group. The ^{13}C NMR spectrum of **5** is also consistent with the assigned structure presented in Figure 3. The FTIR spectrum of **5** shown by Figure 4 demonstrates that

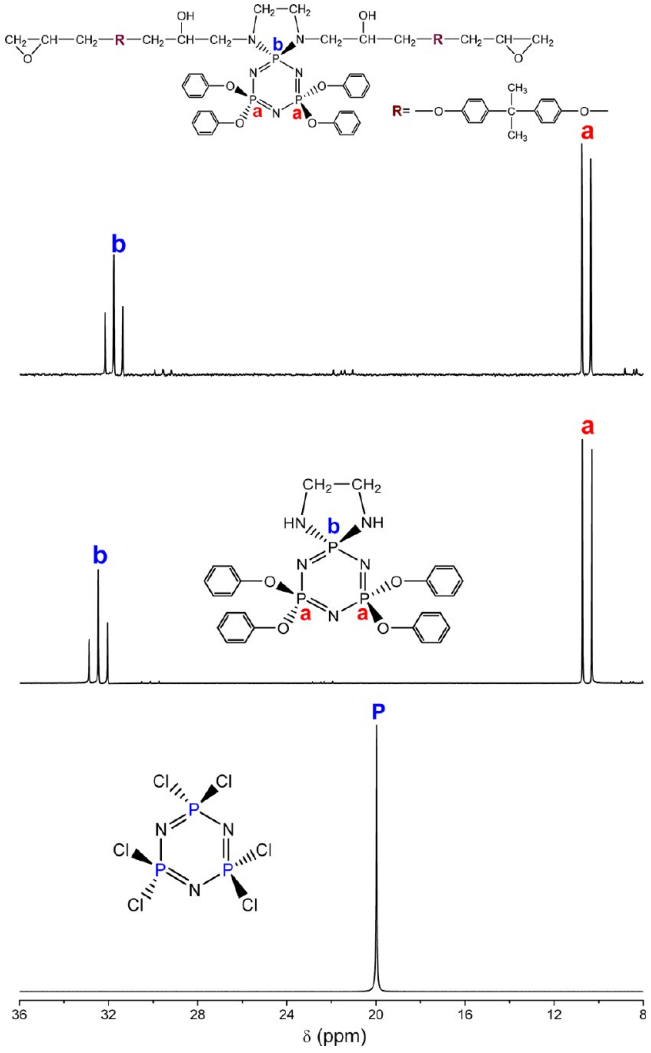

Figure 1. ^{31}P NMR spectra of spiro-cyclotriphosphazene precursor **5** and spirocyclic phosphazene-based epoxy resin **7**.

the appearance of absorption peak at 940 and 1208 cm^{-1} represents the formation of P−O−C bond due to the occurrence of substitution reaction of phenol groups. Meanwhile, a characteristic C−N stretching bond at 1105 cm^{-1} confirms the presence of amino spirocyclic structure. The characteristic absorption peaks corresponding to the aromatic C−H of phenoxy groups are observed at 3067, 1592, 1488, 762, and 684 cm^{-1}. The FTIR spectrum also shows a strong P═N stretching vibration in the infrared spectrum at 1180−1250 cm^{-1}, which is an indication that the phosphazene ring remained intact during the substitution reaction. Furthermore, the mass spectrum shows M^+ at m/z 565.2 consistent with its structure, and the element analysis also confirmed the various

dx.doi.org/10.1021/am300843c | ACS Appl. Mater. Interfaces 2012, 4, 4047−4061

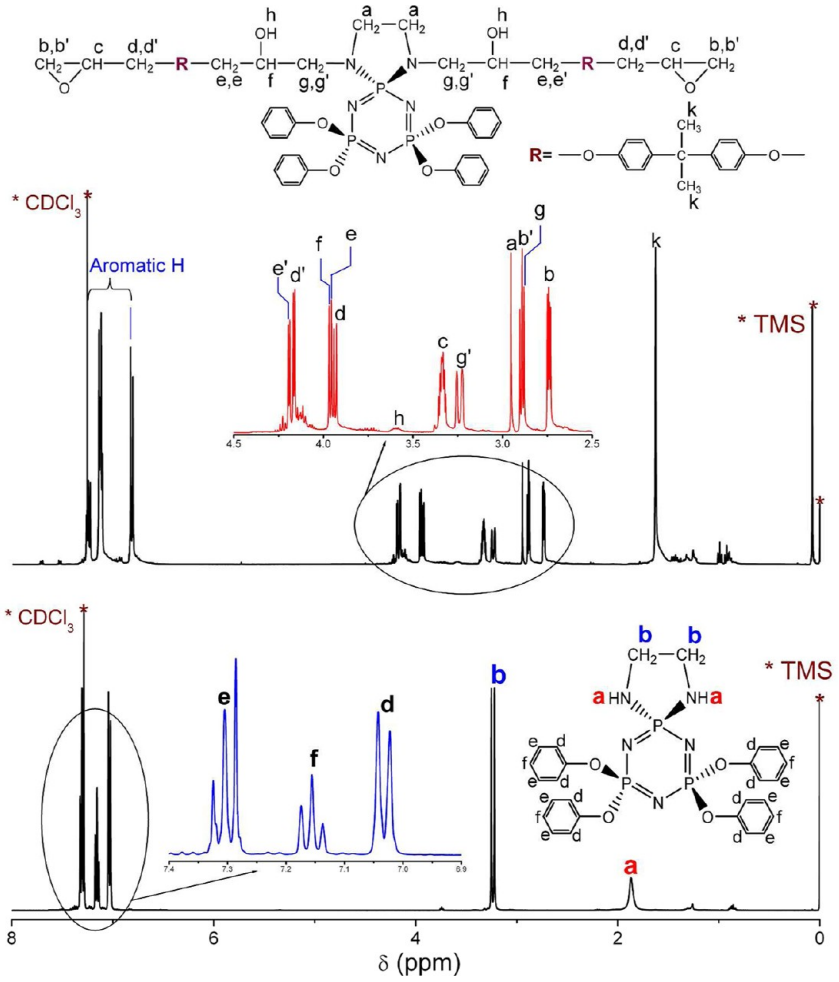

Figure 2. ^{1}H NMR spectra of spiro-cyclotriphosphazene precursor **5** and spirocyclic phosphazene-based epoxy resin **7**.

element ratios in **5**. These characterization results indicate a substitution reaction occurring at two phosphorus atoms of **3** by tetra-phenol groups.

The novel spirocyclic phosphazene-based epoxy resin **7** was synthesized through the polycondensation of the tetraphenoxy-substituted spiro-phosphazene precursor **5** with **6** under the catalysis of TEOA as shown in Scheme 3. The structure of **7** has been determined on the basis of ^{1}H, ^{13}C, and ^{31}P spectroscopy, FTIR spectroscopy, and SEC. The ^{31}P NMR spectrum illustrated in Figure 1 supports the chemical structure of **7**, and the chemical shifts for the substituent phosphorus atoms are in good agreement with those found for **5**. It is interestingly observed from the spectrum of **7** that the triplet resonance signals for the phosphorus atom substituted with a monospiro group is slightly shifted upfield due to the different substituent environment between P*−N $(CH_2)_2$ of **7** and P*−NH(CH_2) of **5**. Figure 2 shows that the ^{1}H NMR of **7** represents a very complex spectrum. Although there are several sets of complicated resonance signals, they are still assigned well to all the protons on the molecular chains of this epoxy resin as labeled and depicted in the inset of Figure 2. The resonance signals corresponding to the aromatic protons appear as three sets of multiplets in the range of 7.4−6.6 ppm, which is a typical region for the benzene rings of both the substituents on cyclotriphosphazene and the backbone. A strong singlet resonance signal at 1.63 ppm is characteristic of the protons (labeled k) of methyl on 4-(2-(4-hydroxyphenyl)-propan-2-yl)phenoxy units (−O−C_6H_6−C$(CH_3$*$)_2$−C_6H_6−O−). As is shown by the inlet of Figure 2, two sets of multiplet resonance signals at around 3.92 and 4.16 ppm corresponding to the protons (labeled d,d′) of the methylene connected with oxirane rings are an indication of the reaction at these site to form the final epoxy resin. The other two sets of multiplet resonance signals at around 2.89 and 2.74 ppm are attributed to the protons (labeled b,b′) of the methylene on oxirane ring, while a set of multiplet resonance signals appear at around 3.33 ppm as the assignment for the protons (labeled c) of methine on oxirane ring. In addition, three sets of weak resonance signals at 3.22, 3.96, and 3.59 ppm, assigned to the protons of methylene [−CH_2*−CH(OH)−CH_2*−], methine [−CH_2−CH*(OH)−CH_2−], and hydroxy [−CH_2−CH-(OH*)−CH_2−] on the molecular backbone, respectively, can also be distinguished from the ^{1}H NMR spectrum of **7**. The ^{13}C NMR spectrum shown in Figure 3 supports the chemical structure of **7** as well. The resonance signals for the substituent carbon atoms are in good agreement with expected chemical shifts for **7** and their assignments were well-labeled and depicted in Figure 3. The FTIR spectrum confirms the composition of **7**. As shown in Figure 4, two distinct absorption peaks appear at 1241 and 1215 cm^{-1} due to the asymmetrical N−P═N stretching while an intensive bond corresponding to the symmetrical stretching vibration of P−N is observed at 855 cm^{-1}, indicating the presence of the phosphazene rings. The characteristic peak at 1175 cm^{-1} is attributed to the P−O−C

dx.doi.org/10.1021/am300843c | ACS Appl. Mater. Interfaces 2012, 4, 4047−4061

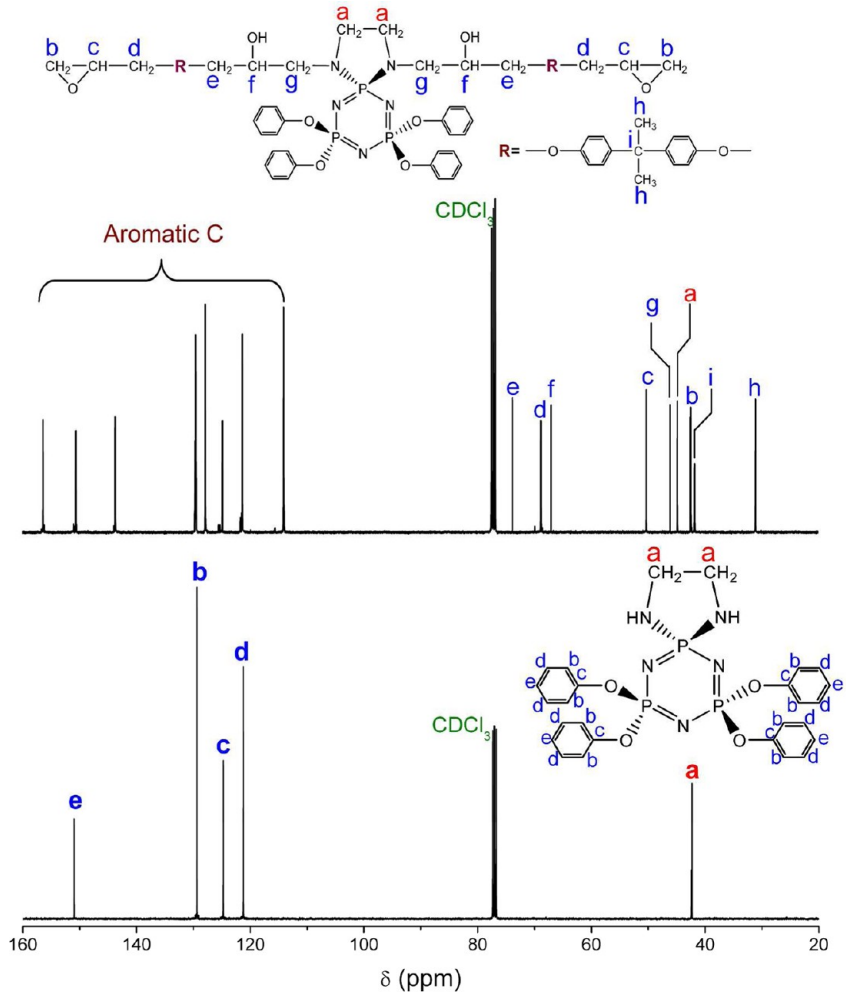

Figure 3. ^{13}C NMR spectra of spiro-cyclotriphosphazene precursor **5** and spirocyclic phosphazene-based epoxy resin **7**.

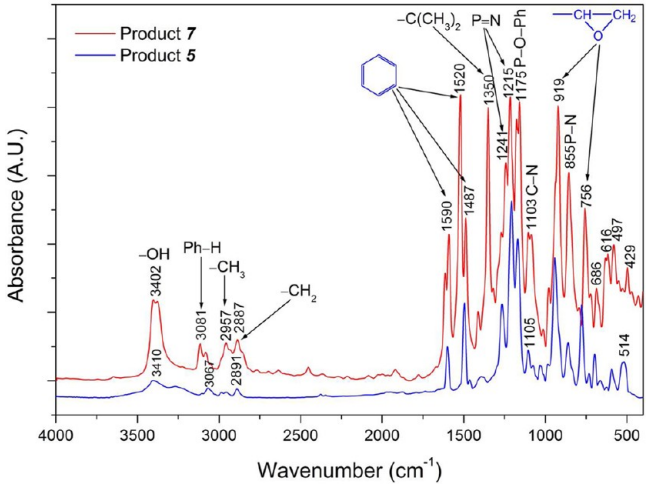

Figure 4. FTIR spectra of spiro-cyclotriphosphazene precursor **5** and spirocyclic phosphazene-based epoxy resin **7**.

bonding. The presence of spiro-amino group is confirmed by a characteristic C−N stretching bond at 1103 cm^{-1} in the IR spectrum. As an important feature of the spectrum, two intensive bands characteristic of oxiranic C−O−C stretching vibration appear at 919 and 756 cm^{-1}. The absorption bands at 3402, 2957, 2887, and 1350 cm^{-1} are attributed to the hydrogen-bonded O−H, $-CH_3$, $-CH_2-$, and $-C(CH_3)_2-$ stretching vibrations, respectively. These results provide an evidence for the incorporation of epoxy groups. The presence of phenoxy groups is also characterized by the characteristic absorption peaks at 3081, 1590, 1520, and 1487 cm^{-1} representative of the aromatic C−H, C−C, and C═C stretching vibrations. In addition, the element analysis result collected in the experimental section further confirmed the chemical composition of **7**.

The GPC data demonstrates that the synthesized epoxy resin has a number-average molecular weight no more than 1285 and a weight-average molecular weight of 1461. The GPC trace also indicates that the most (around 92.14 wt %) of **7** only contains one spirocyclic cyclotriphosphazene unit, and a little (7.25 wt %) of **7** contains two units, but a very small amount of **7** contains three ones or more. Although **7** was synthesized by the reaction of **5** and **6** at a molar ratio of 1:2, it is difficult to obtain the hundred percent of ideal product in a mode of one spirocyclic cyclotriphosphazene unit connecting with two DGEBA moieties. A further condensation between **7** and **5** occurred, and consequently produced a few molecules that contain two or more spirocyclic cyclotriphosphazene units. Therefore, the molecular weight of **7** exhibited polydispersity with an index of 1.137. The EEW of **7** has been determined by the HCl/acetone chemical titration method and shows a value of 674.8 g/equiv. It is noteworthy that the EEW of **7** is very

Scheme 3. Synthetic Reaction for the Formation of Spirocyclic Phosphazene-Based Epoxy Resin 7

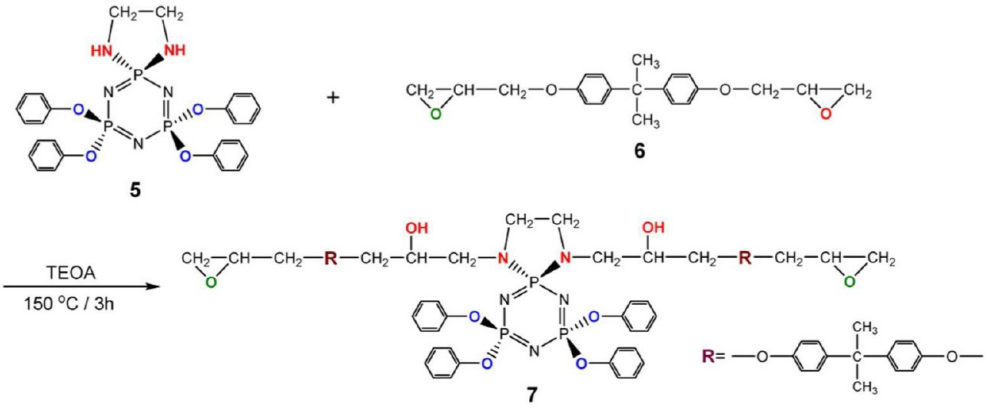

close to its theoretical values of 642.5 g/equiv based on the GPC data, indicating that the reaction between **5** and **6** has been performed completely.

3.2. Thermal Curing Behaviors and Kinetics. Dynamic DSC scans were performed to monitor the nonisothermal curing behaviors of spirocyclic phosphazene-based epoxy resin with DDM, DDS, and novolac. The onset exothermic temperature (T_{onset}), end exothermic temperature (T_{end}), and exothermic peak temperature (T_p) were directly obtained from the dynamic scanning thermograms, and the curve integral was run to calculate the curing heat (ΔH) during overall curing process. Figure 5 shows the dynamic DSC thermograms of these curing systems at various scanning rates, and corresponding data are summarized in Table 1. It is visible that all the curing systems show a single exothermic peak corresponding to the curing reactions of the synthesized epoxy resin with hardeners. This result implies that the thermal curing has performed completely for each curing system without any postcuring as a result of homopolymerization. As seen in Figure 5, the T_{onset}, T_p, and T_{end} for each of these three curing systems shifted to higher temperatures with an increase of heating rate, which is a behavior widely described in the literature.[40,41] This phenomenon indicates that the curing reaction can be accelerated by improving the curing temperature. It is also noteworthy from Table 1 that the T_{onset} of the epoxy resin cured with DDM is lower than the other two curing systems at a given heating rate, indicating that the thermal curing reaction of this curing system occurred initially prior to the other two hardeners. However, the exothermic peak temperature (T_p) corresponding to the curing reaction of spirocyclic phosphazene-based epoxy resin with DDS is much higher that those of the other two curing system, and a trend in terms of T_ps stands by an order of DDS > DDM > novolac at the same heating rates. This result suggests that DDS has a much lower chemical reactivity with the synthesized epoxy resin than the other two hardeners, and furthermore, the chemical reactivity of these three hardeners toward the epoxy resin increases accordingly in the order of novolac > DDM > DDS. Moreover, the curing reaction of the epoxy resin with novolac shows the lowest curing heat among these three curing systems at the given heating rates. This result reflects that novolac is more reactive with spirocyclic phosphazene-based epoxy resin than the other two hardeners, which is consistent with the values of T_p. It is interesting to notice that the curing heat decreases with an increase of heating rate for the curing reactions of the epoxy resin with DDM and DDS, whereas the curing reaction of that with novolac exhibits an opposite trend. Generally, the higher heating rate makes epoxy resin more reactive with hardener. However, in the case of spirocyclic phosphazene-based epoxy resin with novolac, the curing system became less reactive at higher heating rates.

It is an important subject to investigate the curing kinetics of spirocyclic phosphazene-based epoxy resin with various hardeners in order to determine the curing parameters, because the appropriate curing conditions plays an important role in the physical and mechanical properties of epoxy thermosets. Kinetic models developed from kinetic analysis of DSC data have been widely applied to the curing of epoxy resins,[42,43] and kinetics study is usually based on the equation as follows

$$\frac{d\alpha}{dt} = A\exp\left(-\frac{E}{RT}\right)f(\alpha) \quad (1)$$

where α represents the curing degree of epoxy resin, T is the temperature, t is the reaction time, A is the frequency factor, E is the activation energy of curing reaction, R is the gas constant, and $f(\alpha)$ is a model function that depends on the reaction mechanism. Assuming the heat flow is proportional to the change in the extent of curing reaction

$$\frac{d\alpha}{dt} = \frac{1}{\Delta H_0}\frac{dH}{dt} \quad (2)$$

where dH/dt represents the rate of heat generated during curing reaction, and ΔH_0 is the curing heat of overall curing reaction, which can be calculated by running the integral of curing dynamic thermogram. The well-known Kissinger–Akahira–Sunose (KAS) and Flynn–Wall–Ozawa (FWO) methods are usually used to analyze the nonisothermal curing kinetics,[44,45] because the kinetic parameters like E and A can be simply obtained from KAS's and FWO's equations without any assumption about the equation related to reaction conversion. In the case of KAS method, the activation energy (E_k) can be given from the slope of the plot of $\ln(\beta/T_p^2)$ versus $1/T_p$ by the equation as follows:[46]

$$-\ln\left(\frac{\beta}{T_p^2}\right) = -\frac{E_k}{RT_p} - \ln\frac{AR}{E_k} \quad (3)$$

where β is the heating rate during dynamic scan. On the basis of the E_k obtained from the Kissinger–Akahira–Sunose (KAS) method, the Crane method gives a relationship between the β and the curing reaction order (n) and is expressed as follows[47]

dx.doi.org/10.1021/am300843c | ACS Appl. Mater. Interfaces 2012, 4, 4047–4061

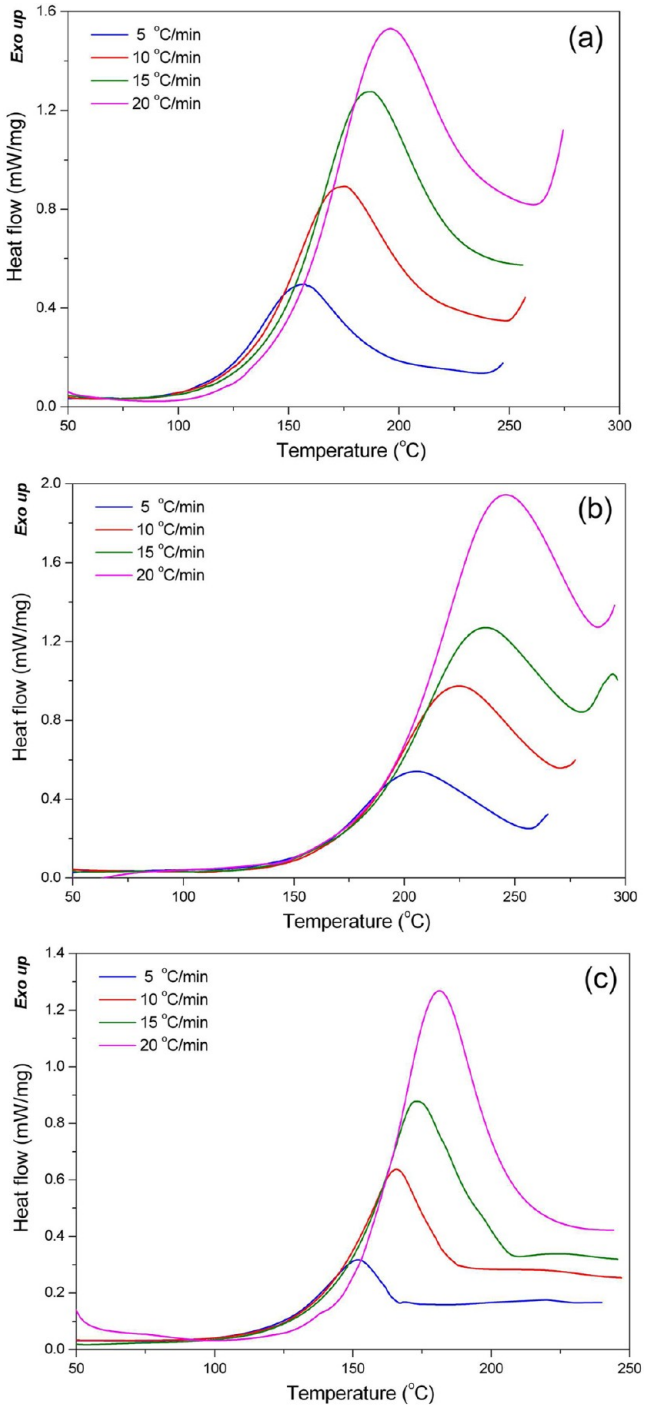

Figure 5. Dynamic DSC scanning thermograms of the thermal curing reactions of spirocyclic phosphazene-based epoxy resin with (a) DDM, (b) DDS, and (c) novolac at different scanning rates.

$$\frac{d(\ln \beta)}{d(1/T_p)} = -\left(\frac{E_k}{nR} + 2T_p\right) \quad (4)$$

As long as the $E_k/(nRT_p)$ is much greater than 2, the n can be derived from the slope of the plot of $\ln\beta$ versus $1/T_p$. Furthermore, the activation energy (E_o) derived from FWO method can also be obtained from the slope of the plot of $\ln\beta$ versus $1/T_p$ according to the FWO's equation expressed as follows:[48]

Table 1. Nonisothermal Curing Parameters Obtained from DSC Analysis for the Curing Reaction of Spirocyclic Phosphazene-Based Epoxy Resin with Three Hardeners

curing system	β (°C/min)	T_{onset} (°C)	T_{end} (°C)	T_p (°C)	ΔH (J/g)
SP-PN epoxy[a]/DDM	5	117.83	234.82	156.15	254.9
	10	130.59	249.19	174.09	228.2
	15	141.04	254.25	184.47	206.6
	20	147.95	262.58	193.73	179.7
SP-PN epoxy[a]/DDS	5	157.18	257.05	202.87	266.9
	10	171.83	269.91	221.59	218.4
	15	179.79	280.53	233.50	207.1
	20	189.28	287.35	241.99	203.3
SP-PN epoxy[a]/novolac	5	124.34	174.74	151.88	64.39
	10	138.36	193.83	165.72	81.64
	15	145.44	207.10	172.67	99.42
	20	151.89	228.42	180.65	112.2

[a]Abbreviation of the spirocyclic phosphazene-based epoxy resin.

$$\ln \beta = -1.052\frac{E_o}{RT_p} + \ln\left(\frac{AE_o}{R}\right) - 5.331 \quad (5)$$

Figure 6 illustrates the Kissinger and Ozawa plots for these three curing systems. The curing kinetic parameters, i.e., E_k, E_o, n, and A, have been obtained from the slopes and intercepts of these plots and are summarized in Table 2. The data regarding the activation energy demonstrate a good agreement between Kissinger and Ozawa methods for these three curing systems. It is observed that the values of both E_k and E_o for three curing systems exhibit a variation trend in an order of novolac > DDS > DDM. Although the curing reaction of spirocyclic phosphazene-based epoxy resin with novolac shows a lowest T_p as mentioned above, it gives the highest reactive activation energy. This means the curing reaction for this system starts earlier, but there is an increase in the potential barrier of the curing reaction in comparison with the other two systems due to the lower temperature range in which the reaction occurs. It is well-known that the epoxy curing is carried out through the nucleophilic substitution reaction, and the activation of oxirane-ring-opening is achieved by proton donors during the course of reaction. Novolac contains much more functional groups, i.e. hydroxyl ones, on its molecule and can catalyze the curing reaction by itself, resulting in an easier occurrence of curing reaction than DDM and DDS. However, such a multifunctional feature generates a barrier for the curing reaction in the later curing stage due to the steric hindrance of aromatic units of novolac, and consequently causes the high activation energy. On the other hand, the amine group has much stronger basicity than hydroxyl group. Therefore, the curing reactions of the epoxy with DDM and DDS achieve an improvement in the curing rates and further an increase in conversion rates as a result of the depression of activation energy. The curing system of the epoxy resin with DDM shows lower activation energy than DDS. Considering the chemical reactivity for the curing reaction between oxirane ring and aromatic amine as a typical nucleophilic substitution reaction, the Sulphone unit on DDS molecule has a stronger electron withdrawing and results in a decline of electron density in the reaction sites. This can lead to a less propensity toward nucleophilic attack in oxirane ring. Therefore, DDM exhibits the lowest activation energy for the curing reaction toward the epoxy resin among these three

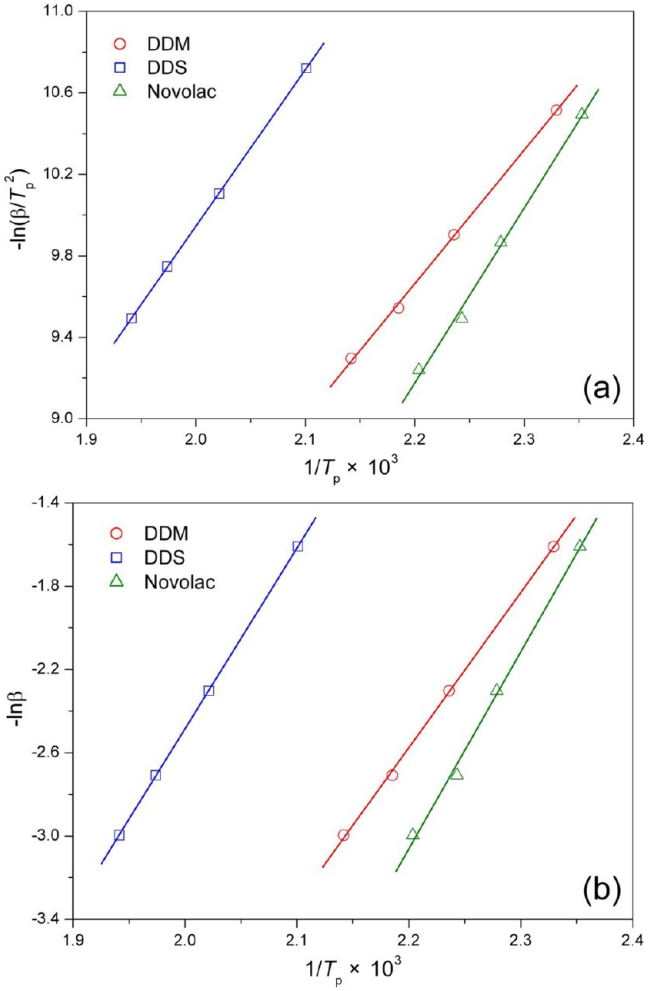

Figure 6. (a) Kissinger's and (b) Ozawa's plots for the curing systems of spirocyclic phosphazene-based epoxy resin with three hardeners.

Table 2. Curing Kinetic Parameters Derived from Kissinger and Ozawa Methods for the Curing Reaction of Spirocyclic Phosphazene-Based Epoxy Resin with Three Hardeners under a Nonisothermal Condition

	Kissinger method			Ozawa method
curing system	E_k (J/mol)	A (s^{-1})	n	E_o (J/mol)
SP-PN epoxy[a]/DDM	54.56	776.53	0.88	58.92
SP-PN epoxy[a]/DDS	63.90	1748.62	0.88	68.56
SP-PN epoxy[a]/novolac	71.39	142329.38	0.91	74.80

[a]Abbreviation of the spirocyclic phosphazene-based epoxy resin.

hardeners. In addition, it is interestingly observed from Table 2 that the reaction orders of these three curing systems are similar and are all less than one, indicating that the curing process is complicatedly but follows the same mechanism. However, the frequency factors of these three curing systems show a strong dependence on the nature of hardeners. It is proposed that the greatest value of the frequency factor for the curing system of the epoxy resin with novolac is attributed to highly efficient initiation of the numerous hydroxyl groups on the novolac molecules for the curing reaction. These proton donors cause the stimulation of the ring-opening procedure and generate an autocatalyzing effect on the curing reaction. On the basis of the above curing kinetic results, it is concluded that these three hardeners take part in the curing reaction with spirocyclic phosphazene-based epoxy resin in a different way and to a different extent, resulting in the different structural characteristics and physical properties of the resulting thermosets.

3.3. Thermal Resistance and Stability. The thermal resistance is one of the most important properties of epoxy thermosets because it establishes the service environment for the epoxy-based functional materials. Usually, glass transition temperature (T_g) is an important parameter of the thermal property of epoxy thermosets, which are only used well, in most cases, at a temperature below T_g. Moreover, T_g is also a parameter that gives the information about the structure of cross-linked epoxy thermosets. Therefore, it is very important for the epoxy resin to achieve a high T_g when designing its molecular structure. The T_gs of spirocyclic phosphazene-based epoxy thermosets cured with three hardeners were evaluated by DSC. Figure 7 shows their DSC thermograms, and the

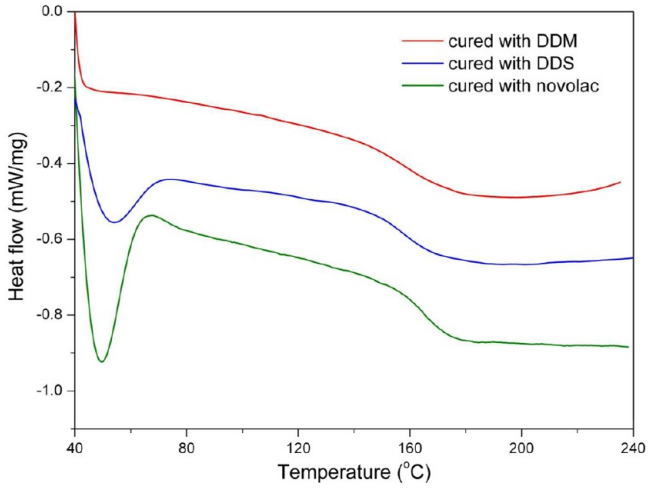

Figure 7. DSC thermograms of spirocyclic phosphazene-based epoxy thermosets cured with three hardeners.

obtained results are summarized in Table 3. It is expected that all the thermosets show a high T_g more than 150 °C, indicating an excellent thermal resistance for the thermosets based on the synthesized epoxy resin. It is well-known that glass transition is generally ascribed to the segmental motion of the polymeric networks, and T_g is determined by the degree of freedom for the segmental motion, cross-linking and entanglement constraints, and the packing density of the segments.[42] In this work, cyclotriphosphazene rings were incorporated into the backbone of the synthesized epoxy resin in the way of linking to the spiro-side group of spirocyclic cyclotriphosphazene. Because the thermal motion of network in glassy state is believed to include the vibration of side group and the motion of cross-linking segment, the pendent cyclotriphosphazene groups on the side of backbones leads to a great steric hindrance and thus confines these motions. This increases the dimensional stability of the cured epoxy resins at elevated temperature and improves the T_gs of spirocyclic phosphazene-based epoxy thermosets. It is also observed that the epoxy thermoset achieved a much higher T_g when cured with novolac compared to the other two hardeners. As is well-known, novolac contains more reactive groups for cross-linking than DDM and DDS. This resulted in a high packing density for the polymeric networks, and thus, a high T_g was gained.

dx.doi.org/10.1021/am300843c | ACS Appl. Mater. Interfaces 2012, 4, 4047−4061

Table 3. Thermal Analysis Results Obtained from DSC and TGA Measurements for Spirocyclic Phosphazene-Based Epoxy Thermosets Cured with Three Hardeners

		nitrogen atmosphere			air atmosphere		
thermoset sample	T_g (°C)	T_{onset}[b] (°C)	T_{max}[c] (°C)	char yield at 750 °C (w %)	T_{onset}[b] (°C)	T_{max}[c] (°C)	char yield at 750 °C (wt %)
SP-PN epoxy[a]/DDM	157.65	287.43	329.90	31.01	291.09	324.01	38.01
SP-PN epoxy[a]/DDS	159.82	315.52	324.78	38.48	311.07	314.88	38.37
SP-PN epoxy[a]/Novolac	164.59	286.92	340.21	36.30	302.85	343.36	34.96

[a]Abbreviation of the spirocyclic phosphazene-based epoxy resin. [b]Onset decomposition temperature, at which the thermoset undergoes 3 wt % weight loss. [c]Characteristic temperature, at which maximum rate of weight loss occurs.

Nevertheless, the thermoset cured with DDS shows a higher T_g than that with DDM. It is reasonable to believe that the rotational hindrance of the Sulphone unit on DDS molecule restricts the segmental motion, and consequently results in a higher T_g for the thermoset.

The thermal stabilities of spirocyclic phosphazene-based epoxy thermosets cured with three hardeners were investigated by TGA under both air and nitrogen atmospheres. Figure 8

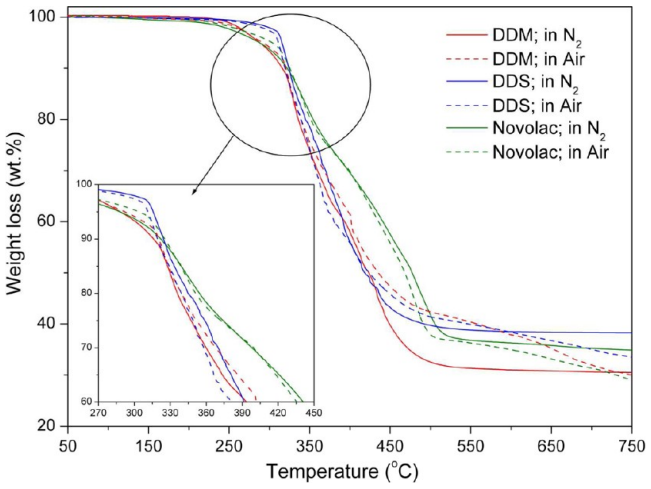

Figure 8. TGA thermograms of spirocyclic phosphazene-based epoxy thermosets cured with three hardeners.

demonstrates the TGA thermograms of these thermosets, and the analysis results are summarized in Table 3. It is obvious that the TGA traces for the thermosets cured with three hardeners present a typical one-stage degradation, indicating that these thermosets underwent one-stage decomposition for the major components of the polymeric networks. The temperature corresponding to 3 wt.% weight loss is defined as a onset decomposition temperature (T_{onset}) and furthermore taken as an index of thermal stability. The TGA results also demonstrate that the T_{onset}s of all the thermosets are in the ranges of 290−310 °C in air and 280−320 °C in nitrogen. It is noteworthy that the main degradation started at a maximum decomposition temperature (T_{max}) beyond 320 °C, at which the weight loss occurred at a maximum rate. Furthermore, it is notable from Table 3 that the characteristic decomposition temperatures in air are similar to those in nitrogen. These results indicate that the spirocyclic phosphazene-based epoxy resin synthesized in this work has a good thermal stability in natural. It should be pointed out that the thermoset cured with DDS shows both a higher onset decomposition temperature and a higher maximum decomposition temperature than those with DDM and novolac. This may be ascribed to the Sulphone structure of DDS, which can endure a higher decomposition temperature. Additionally, the thermoset cured with novolac exhibits a higher T_{max} than that with DDM. This result is attributed to the high cross-linking density of thermoset as well as the thermally stable aromatic units on the molecular backbone of novolac.

As shown by the data in Table 3, the thermoset cured with DDS shows the highest char yields of 38.37 wt % in air and 38.48 wt % in nitrogen among these three samples. The thermoset cured with novolac and DDM also obtained high char yields more than 30 wt % both in air and in nitrogen. The achievement of such high char yields may be due to the highly thermally stable phosphazene rings in the thermosets, which promotes the char formation during the thermal degradation. Furthermore, most of the thermosets exhibit similar char yields both in nitrogen and in air. It is interestingly noted that the thermoset cured with DDM achieved a high char yield of 38.01 wt % in air but only 31.01 wt % in nitrogen. It is understandable that the oxygen in air can enhance the thermooxidative decomposition of the thermosets. However, the most of the oxides of phosphorus in cyclotriphosphazene units are solid, and these phosphorus oxides remain in solid phase, i.e. the residual char during thermooxidative decomposition. Furthermore, the oxidation of sulfur element in DDS and nitrogen one in DDM can also enhance the char formation. Consequently, the decompositions of the thermosets in air resulted in a higher char yield than those in nitrogen. In the case of the thermoset cured with novolac, the novolac as a hardener is a carbohydrate compound, so its cured thermoset decomposes more easily in air than that cured with DDM or DDS. This resulted in a lower char yield in air than that in nitrogen. In addition, the thermoset cured with novolac obtained a higher char yield than that with DDM in nitrogen, which indicates that the high cross-linking density of the thermoset dominates the formation of char in the absence of oxygen. On the basis of these results, it can be deduced that the spirocyclic phosphazene-based epoxy resin is superior in fire and heat resistance compared to other known phosphorus-containing epoxy resins that have been reported.[17,18,34,35]

3.4. Flammability Characteristics. The flame-retardant performance of the thermosets based on spirocyclic phosphazene-based epoxy resin with three hardeners has also been investigated in terms of the LOI and UL−94 vertical burning tests, and the results are summarized in Table 4. As is well-known, LOI measures the minimum oxygen concentration of flowing gas mixed by oxygen and nitrogen required supporting downward flame combustion, which can be used as an indicator to evaluate the flame retardancy of the thermosets. It is expected that all the thermosets exhibit the high values of LOI beyond 29 vol.%, equal to the oxygen concentration of air. This means these thermosets should almost be nonflammable in air, though the LOI values varied a little when the thermosets were cured with different hardeners. This indicates that the incorporation of spiro-cyclotriphosphazene unit into the

Table 4. Flame-Retardant Performance of Spirocyclic Phosphazene-Based Epoxy Thermosets Cured with Three Hardeners

		flammability from vertical burning testing			
thermoset sample	LOI value (vol %)	UL−94 classification	flaming drips	total flaming time (s)	maximal flaming time (s)
SP-PN epoxy[a]/DDM	31.12	V−0	none	28.6	7.7
SP-PN epoxy[a]/DDS	32.54	V−0	none	25.8	6.4
SP-PN epoxy[a]/novolac	30.76	V−0	none	41.8	9.1

[a]Abbreviation of the spirocyclic phosphazene-based epoxy resin.

backbone of epoxy resin as a pendent group is very effective for the enhancement of flame retardancy and makes this epoxy resin become a nonflammable functional polymer. The UL−94 vertical burning test determines the upward burning characteristics of spirocyclic phosphazene-based epoxy thermosets, and the test results are also collected in Table 4. As was expected, all the thermosets achieved a UL94 V−0 classification in UL−94 test. Most of the testing bars quenched within 5−6 s when flame agitator was removed during the vertical burning test, indicating an autoextinguishable feature. Furthermore, the burned residues of these thermosets did not fall off during the vertical burning as a result of the good structural stability of all the thermosets. Such a feature seems to indicate the formation of a protective viscous char layer which sticks to the surface of the thermoset instead of flowing away as it does for the conventional epoxy resins. In order to visually recognize the burning characteristics of the spirocyclic phosphazene-based epoxy resin synthesized in this study, we simulated the UL−94 vertical burning test for a spirocyclic phosphazene-based epoxy thermoset and recorded the whole burning process by digital camera, whereas the combustion of a conventional epoxy thermoset was carried out as a reference. Figure 9 demonstrates the typical burning procedures for the spirocyclic phosphazene-based epoxy thermoset as well as the conventional epoxy one. It is surprisingly noted that, compared to the conventional epoxy thermoset exhibiting a highly combustible behavior, the spirocyclic phosphazene-based epoxy one did not perform an aggressive combustion when contacted by a flame of Bunsen burner for a long-term, whereas the emission of few smoke and no flaming drips were observed during combustion as well. One of the fascinating characteristics of combustion is that this thermoset just combusted slightly with a small blaze and was extinguished quickly by itself within 7 s after contacted by the flame for 10 s. It is interesting to observe that the surface of this thermoset has been covered with an expanded char layer by the end of combustion. This phenomenon implies that this char layer plays a critical role in the fire resistance of the thermoset, and it serves as a protect layer for insulating the underlying material from heat source and preventing heat transfer and flame spread during combustion. These results give a visible evidence of good flame retardancy for the spirocyclic phosphazene-based epoxy thermosets.

It is noteworthy that the spirocyclic phosphazene-based epoxy thermosets cured with DDM and DDS achieved better flame-retardant performance than that with novolac in terms of the LOI and UL−94 testing data. This result is ascribed to the contribution of nitrogen and sulfur elements to the flame retardancy of thermosets when the nitrogen- and sulfur-containing hardeners are employed to cure with spirocyclic phosphazene-based epoxy resin. On the basis of these results, it is evident that the spirocyclic phosphazene-based epoxy has a virtually nonflammable nature. Such good flame retardancy is attributed to the presence of unique combination of phosphorus and nitrogen in the thermosets as a result of directly linking cyclotriphosphazene to the backbone of epoxy resin in a pendent mode. This particular spirocyclic phosphazene-based structure has several advantages for the synthesized epoxy resin to achieve good fire-resistance as well as high performance. First, the amino-spirocyclic cyclotriphosphazene unit of this epoxy resin contains much higher weight percent of inert nitrogen element than the common cyclotriphosphazene-containing epoxy ones. This can impart better flame retardancy to the resulted epoxy resin.[49] Second, the amino-spirocyclic structure is more thermally stable, which leads to a higher thermal stability of the thermosetting system. Finally, a ring-opening reaction to yield polyphosphazenes or a ring expansion to higher cyclic species may occur when the amino-spirocyclic cyclotriphosphazene moieties are heated to a temperature above 250 °C.[50] Such a ring expansion/polymerization reaction can offer a much higher thermal stability and thus much better flame retardancy for the thermosetting

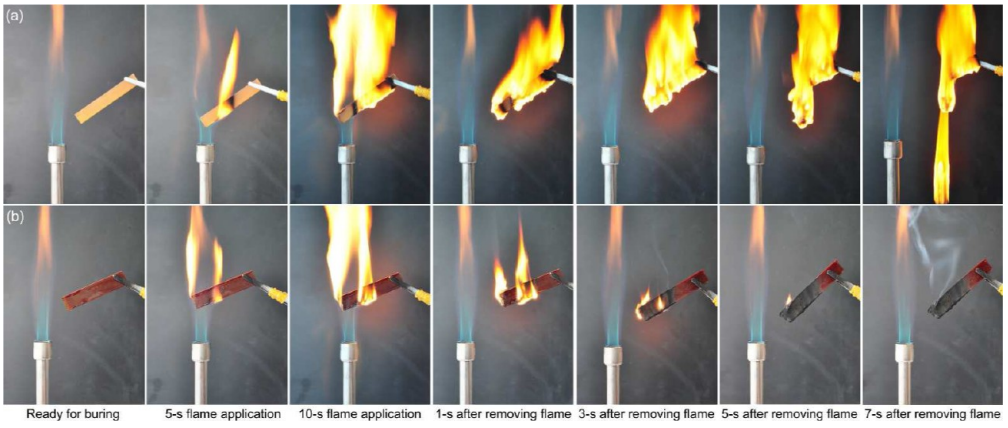

Figure 9. Digital photographs of the combustion procedures of (a) conventional DGEBA-type epoxy thermoset and (b) spirocyclic phosphazene-based epoxy thermosets under a vertical burning condition.

system. Therefore, this characteristic spirocyclic molecular structure is highly advantageous to the reactive flame retardancy induced by the synergistic effect of phosphorus and nitrogen.

3.5. Analysis of Residual Char. Usually, the residual chars formed during combustion can give some important information regarding the inherent flammability characteristics of a polymeric material, and they also reflect the fire-resistant mechanisms to some extent. Therefore, to understand better the char formation of spirocyclic phosphazene-based epoxy thermosets and to learn more about their flame-retardant mechanisms, the morphologies of the residual chars collected from the vertical burning tests were investigated by SEM. Figures 10 and 11 illustrate the SEM images of the outside aspects and inside structures of these residual chars, respectively. As seen in these SEM images, all of these residual chars exhibits some irregular-shaped and multiporous bulks, and the inside of the chars shows a honeycomb structure according to the magnified micrographs of each sample, indicating a typical morphology after the intumescent char formation. Furthermore, the outside aspects of these residual chars illustrate a very gassy surface without any pores breaking through as shown in Figure 10. It is well-known that the physical structure of the charring layer plays a very important role in the performance of flame retardancy. From the observation of the residual chars of the spirocyclic phosphazene-based epoxy thermosets, the char layer formed during combustion is rigid and compact in nature, and there are lots of integrated closed honeycomb pores inside. Such a structural form favors the temperature grads in the char layer and protects the matrix inside. Therefore, it is concluded that the thermooxidative reaction of cyclotriphosphazene moieties enhances the char formation during combustion, which results in a protective char layer formed on the surface of thermosets serving as a barrier against heat and oxygen diffusion, and consequently the flame retardancy of the thermosets is improved significantly. In addition, it should be highly noted that the char structure of the thermoset cured with novolac seems to be much more loose and porous than those with DDM and DDS, which leads to a collapse of some pore walls as observed in Figure 11c. As is mentioned previously by the TGA data, the thermoset cured with novolac is much easier to decompose thermooxidatively with lower char yield than the other two thermosets. In this case, this thermoset generates much more gaseous products during combustion, consequently resulting in the formation of seriously multiporous chars. Such an excessively multiporous structure is disadvantageous for the prevention of heat transfer and flame spread during combustion when retarding flame. This feature is in a good agreement with the results of the LOI and UL−94 vertical burning tests.

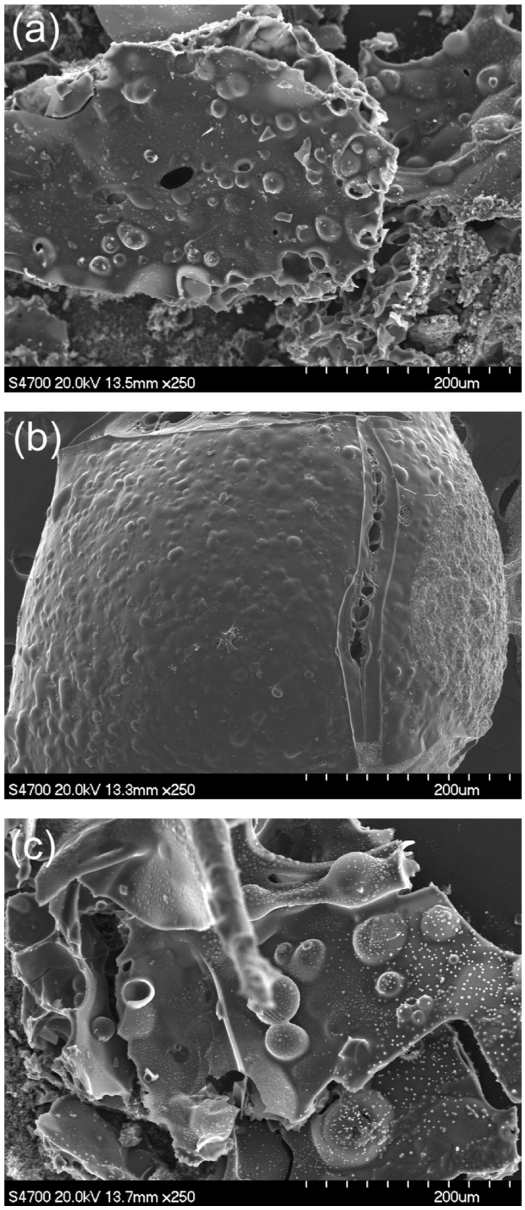

Figure 10. SEM images of the outside aspects of residual chars obtained from the vertical burning tests for spirocyclic phosphazene-based epoxy thermosets cured with (a) DDM, (b) DDS, and (c) novolac.

The chemical compositions of residual chars were further investigated by FTIR spectroscopy. Figure 12 shows the FTIR spectra of the residual chars collected from three thermosets after UL−94 vertical burning tests were completed. It seems that the three spectra present the similar patterns of highly carbonized compounds, indicating these residual chars have a similar chemical structure. As seen in Figure 12, a series of absorption peaks at 1620, 1544, and 1396 cm^{-1} can be attributed to the carbonized networks like aromatics and polyaromatics formed during the combustion. A broad absorption of P−O−C bond appears at around 1093 cm^{-1}, suggesting that the residual chars contain phosphorus oxides together with carbon ones. A weak characteristic band at 2924 cm^{-1} is due to the organic part of the char and does not refer to the low content of the organic species in the char, because carbonized phosphorus-rich pyrolysis products absorbs much more strongly. A broad peak is observed in the region of 3500−3000 cm^{-1}, which is attribute to the stretching vibration of O−H and N−H bond. This indicates that the pyrolysis products of the thermosets include water and the other hydroxy and amino compounds derived from cyclotriphosphazene pyrolysis. Additionally, the appearance of an absorption band at 978 cm^{-1} is attributed to the −C═C− wagging vibration resulting from the carbonized pyrolysis products of the thermosets. These results indicate that the residual chars mainly consist of cross-linked phosphorocarbonaceous and phosphorooxidative solids as well as highly carbonized aromatic networks.

On the basis of the investigation of the physical structure and chemical composition of residual chars, it can be deduced that

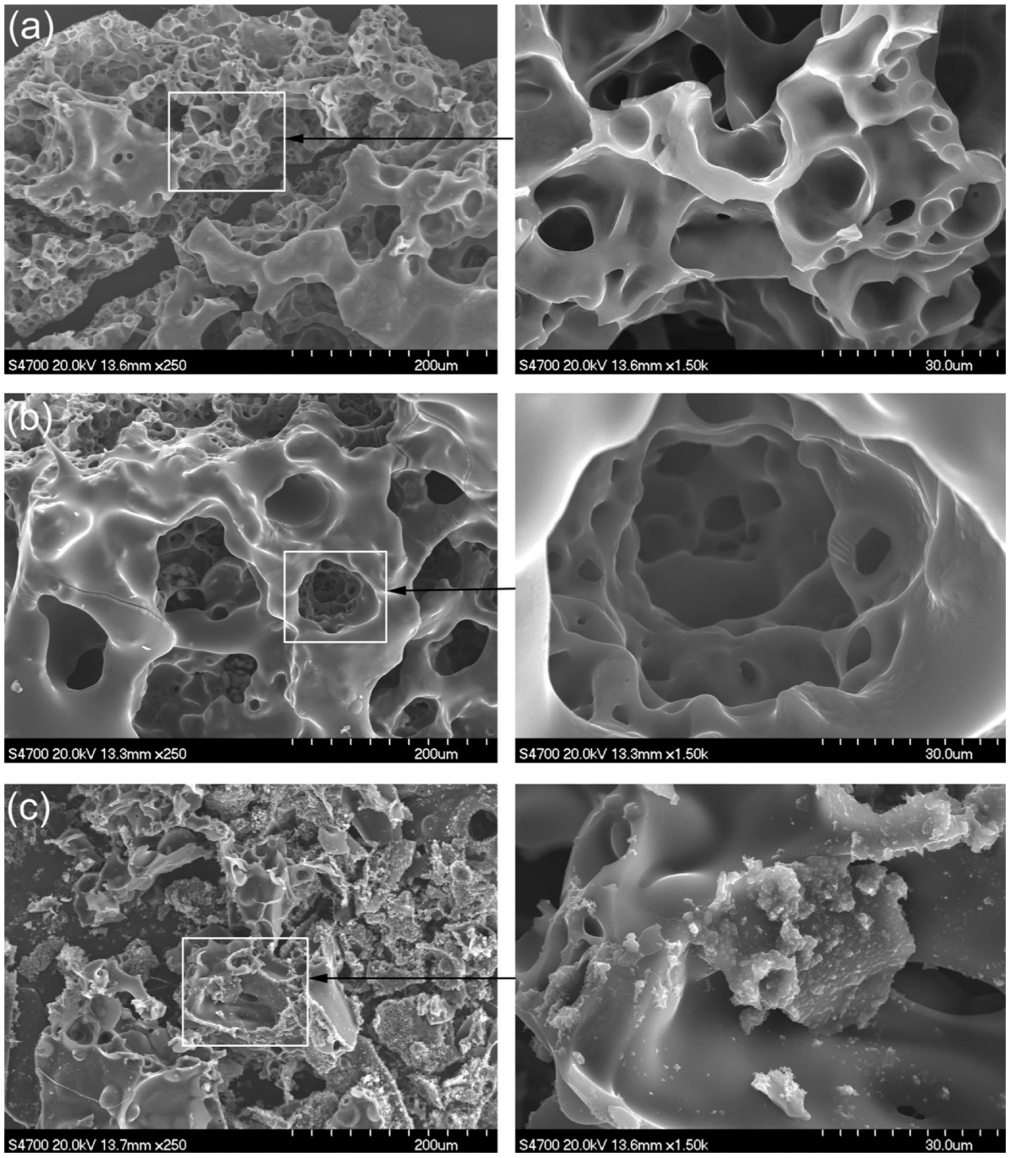

Figure 11. SEM images of the inside structures of residual chars obtained from the vertical burning tests for spirocyclic phosphazene-based epoxy thermosets cured with (a) DDM, (b) DDS, and (c) novolac.

the achievement of nonflammability of the spirocyclic phosphazene-based epoxy resin results from the inherent flame retardancy of spiro-cyclotriphosphazene moieties due to its synergistic effect of phosphorus−nitrogen combination. Although the flame-retardant mechanism of phosphazene-based polymers like the epoxy resin synthesized in this work is still not very clear, it is concluded that the presence of spiro-cyclotriphosphazene moieties on the backbone of the epoxy resin enhances the flame retardancy in the ways of both condensed and gaseous phases.[51−53] The thermooxidative reaction of phosphazene rings with the other segments can form phosphorus-rich char on the surface as a barrier to prevent gaseous products from diffusing to the flame and to shield the polymer surface from heat and air during combustion. Simultaneous, the pyrolysis of phosphazene rings can produces phosphoric or polyphosphoric acid, which acts in the condensed phase promoting char formation. On the other hand, the cyclotriphosphazene moieties can release nonflammable gases such as CO_2, NH_3 and N_2 during combustion to dilute the hot atmosphere and cool the pyrolysis zone at the combustion surface. The aforementioned inflammable gases can cut off the supply of oxygen, and thus leads to the autoextinguishability of the thermosets. Nevertheless, the effect of the molecular structures of phosphazene-based epoxy functional polymers and their participation in all stages of combustion process are not fully understood yet. A further intensive study is still necessary to explore the relationship between the molecular structure and the flame retardancy for phosphazene-based epoxy functional polymers, so that more favorable molecular structure can be designed for the corresponding polymers to obtain much better flame retardancy and much higher performance.

4. CONCLUSIONS

A novel halogen-free flame-retardant epoxy resin with spirocyclic phosphazene-based structure was synthesized successfully in good yields through a three-step reaction pathway. The chemical structures and compositions of all the intermediate and final products were confirmed by ^{1}H, ^{13}C, and ^{31}P NMR spectroscopy, elemental analysis, mass spectroscopy,

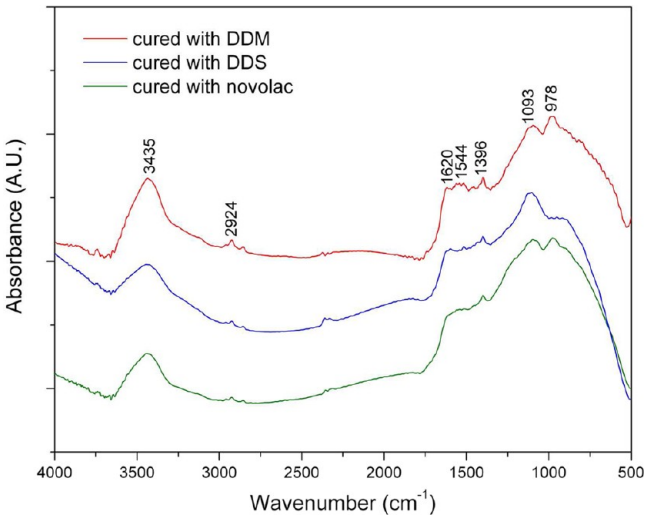

Figure 12. FTIR spectra of the residual chars collected from the vertical burning tests for spirocyclic phosphazene-based epoxy thermosets cured with three hardeners.

and FTIR spectroscopy. The thermosets of this epoxy resin cured with DDM, DDS, and novolac as hardeners achieved a high thermal resistance due to their high T_gs over 150 °C, and they also obtained good thermal stabilities with high char yields. The incorporation of spiro-cyclotriphosphazene units into the backbone imparts fire resistance to the synthesized epoxy resin because of the unique combination of phosphorus and nitrogen following by a synergistic effect on flame retardancy. The pyrolysis products of cyclotriphosphazene moieties acted in both the condensed and gaseous phases to promote the formation of intumescent and compact char on the surface of polymers. Such a char layer can supply a much better barrier for underlying polymer to inhibit gaseous products from diffusing to the flame, to shield the polymer surface from heat and air, and to prevent or slow down oxygen diffusion. As a result, all the thermosets based on this epoxy resin achieved high LOI values and UL−94 V−0 classification. The epoxy resin synthesized in this study will be a potential candidate as a green functional material for fire- and heat-resistant applications in electronic and microelectronic fields with more safety and excellent performance.

AUTHOR INFORMATION

Corresponding Author

*Tel: +86 10 6441 0145. Fax: +86 10 6442 1693. E-mail: wangxdfox@yahoo.com.cn.

Notes

The authors declare no competing financial interest.

ACKNOWLEDGMENTS

The financial support from the National Natural Science Foundation of China (Project Grant 50973005) is gratefully acknowledged.

REFERENCES

(1) Wan, J.; Li, C.; Bu, Z.; Xu, C.; Li, B. *Chem. Eng. J.* **2012**, *188*, 160.
(2) Nakamura, Y.; Yamaguchi, M.; Okubo, M.; Matsumoto, T. *J. Appl. Polym. Sci.* **1992**, *45*, 1281.
(3) Pecht, M.; Deng, Y. *Microelectron. Reliab.* **2006**, *46*, 53.
(4) Sun, D.; Yao, Y. *Polym. Degrad. Stab.* **2011**, *96*, 1720.
(5) Lu, S.; Hamerton, I. *Prog. Polym. Sci.* **2002**, *27*, 1661.
(6) Mauerer, O. *Polym. Degrad. Stab.* **2005**, *88*, 70.
(7) Qian, L.; Ye, L.; Xu, G.; Liu, J.; Guo, J. *Polym. Degrad. Stab.* **2011**, *96*, 1118.
(8) Guo, Y.; Qiu, J.; Tang, H.; Liu, C. *J. Appl. Polym. Sci.* **2011**, *121*, 727.
(9) Toldy, A.; Toth, N.; Anna, P.; Marosi, G. *Polym. Degrad. Stab.* **2006**, *91*, 585.
(10) Wang, X.; Song, Lei.; Xing, W.-Y.; Lu, H.-D.; Hu, Y. *Mater. Chem. Phys.* **2011**, *125*, 536.
(11) Gao, F.; Tong, L.; Fang, Z. *Polym. Degrad. Stab.* **2006**, *91*, 1295.
(12) Sun, S.; He, Y.; Wang, X.; Wu, D. *J. Appl. Polym. Sci.* **2010**, *118*, 611.
(13) Thirumal, M.; Khastgir, D.; Nando, G. B.; Naik, Y. P.; Singha, N. K. *Polym. Degrad. Stab.* **2010**, *95*, 1138.
(14) Gaan, S.; Sun, G.; Hutches, K.; Engelhard, M. H. *Polym. Degrad. Stab.* **2008**, *93*, 99.
(15) Thirumal, M.; Singha, N. K.; Khastgir, D.; Manjunath, B. S.; Naik, Y. P. *J. Appl. Polym. Sci.* **2010**, *116*, 2260.
(16) Kang, N.; Du, Z.; Li, H.; Zhang, C. *Polym. Adv. Technol.* **2011**, *22*, 1099.
(17) Shieh, J.; Wang, C. *J. Polym. Sci., Part A: Polym. Chem.* **2002**, *40*, 369.
(18) Gao, L.; Wang, D.; Wang, Y.; Wang, J.; Yang, B. *Polym. Degrad. Stab.* **2008**, *93*, 1308.
(19) Schartel, B.; Braun, U.; Artner, J.; Ciesielski, M.; Doring, M.; Altstadt, V. *Eur. Polym. J.* **2008**, *44*, 704.
(20) Ren, H.; Sun, J.; Wu, B.; Zhou, Q. *Polym. Degrad. Stab.* **2007**, *92*, 956.
(21) Chen, H.; Zhang, Y.; Chen, L.; Shao, Z.; Liu, Y.; Wang, Y. *Ind. Eng. Chem. Res.* **2010**, *49*, 7052.
(22) Jeng, R. J.; Shau, M.; Lin, J. J.; Su, W. C.; Chiu, Y. S. *Eur. Polym. J.* **2002**, *38*, 68.
(23) Kandola, B. K.; Biswas, B.; Price, D.; Horrocks, A. R. *Polym, Degrad. Stab.* **2010**, *95*, 144.
(24) Liu, R.; Wang, X. *Polym. Degrad. Stab.* **2009**, *94*, 617.
(25) Chen-Yang, Y. W.; Yuan, C. Y.; Li, C. H.; Yang, H. C. *J. Appl. Polym. Sci.* **2003**, *90*, 1357.
(26) Diefenbach, D.; Allcock, H. R. *Inorg. Chem.* **1994**, *33*, 4562.
(27) Chandrasekh ar, V.; Krishnan, V. *Adv. Inorg. Chem.* **2002**, *53*, 159.
(28) De Jaeger, R.; Gleria, M. *Prog. Polym. Sci.* **1998**, *23*, 179.
(29) Allcock, H. R. J. Inorg. *Organomet. Polym. Mater.* **2007**, *17*, 349.
(30) Chen-Yang, Y. W.; Cheng, S. J.; Tsai, B. D. *Ind. Eng. Chem. Res.* **1991**, *30*, 1314.
(31) Allcock, H. R. J. Inorg. *Organomet. Polym. Mater.* **2006**, *16*, 277.
(32) Ding, J.; Shi, W. *Polym. Degrad. Stab.* **2004**, *84*, 159.
(33) Xu, J.; Toh, C. L.; Ke, K. *Macromolecules* **2008**, *41*, 9624.
(34) Wang, X.; Zhang, Q. *Eur. Polym. J.* **2004**, *40*, 385.
(35) Chen-Yang, Y. W.; Lee, H. F. *J. Polym Sci, Part A: Polym. Chem.* **2000**, *38*, 972.
(36) Buckingham, M. R.; Lindsay, A. J.; Stevenson, D. E.; Muller, G.; Morel, E.; Costes, B.; Henry, Y. *Polym. Degrad. Stab.* **1996**, *54*, 311.
(37) Kumar, D.; Fohlen, G. M.; Parker, J. A. *J. Polym. Sci., Part A: Polym. Chem.* **1986**, *24*, 2415.
(38) Fushimi, T.; Allcock, H. R. *Dalt. Trans.* **2010**, *39*, 5349.
(39) Zhang, J.; Zheng, H.; Bi, Y. *Struct. Chem.* **2008**, *19*, 297.
(40) Menczel, J. D.; Prime, R. B. *Thermal Analysis of Polymers: Fundamentals and Applications*; John Wiley & Sons: Hoboken, NJ, 2009.
(41) Haines, P. J. *Principles of Thermal Analysis and Calorimetry*; The Royal Society of Chemistry: Cambridge, U.K., 2002.
(42) Wang, H.; Zhang, Y.; Zhu, L.; Du, Z.; Zhang, B.; Zhang, Y. *Thermochim. Acta* **2012**, *529*, 29.
(43) Sbirrazzuoli, N.; Vyazovkin, S.; Mititelu, A.; Sladic, C.; Vicent, L. *Macromol. Chem. Phys.* **2003**, *204*, 1815.
(44) Kissinger, H. E. *Anal. Chem.* **1957**, *29*, 1702.
(45) Ozawa, T. *Bull. Chem. Soc. Jpn.* **1965**, *38*, 1881.
(46) Liu, W.; Qiu, Q.; Wang, J.; Huo., Z.; Sun, H. *Polymer* **2008**, *49*, 4399.

(47) Crane, L. W.; Dynes, P. J.; Kaelble, D. H. *J. Polym. Sci., Polym. Lett. Ed.* **1973**, *11*, 533.
(48) Jubsilp, C.; Damrongsakkul, S.; Takeichi, T.; Rimdusit, S. *Thermochim. Acta* **2006**, *477*, 131.
(49) Liu, J.; Wang, X.; Wu, D. *RSC Adv.* **2012**, *2*, 5789.
(50) Allcock, H. R.; Diefenbach, D.; Pucher, S. R. *Inorg. Chem.* **1994**, *33*, 3091.
(51) Nie, S.; Hu, Y.; Song, L.; He, Q.; Yang, D.; Chen, H. *Polym. Adv. Technol.* **2008**, *19*, 1077.
(52) Laoutid, F.; Bonnaud, L.; Alexandre, M.; Lopez-Cuesta, J.; Dubois, P. *Mater. Sci. Eng., R* **2009**, *63*, 100.
(53) Levchik, S. V.; Weil, E. D. *J. Fire Sci.* **2006**, *24*, 345.